Electronic Supplementary Information for

"Depolarization of Few-Layer III-V and II-VI Materials through Symmetric

Rumpling"

An-An Sun and Shang-Peng Gao*

Department of Materials Science, Fudan University, Shanghai 200433, China
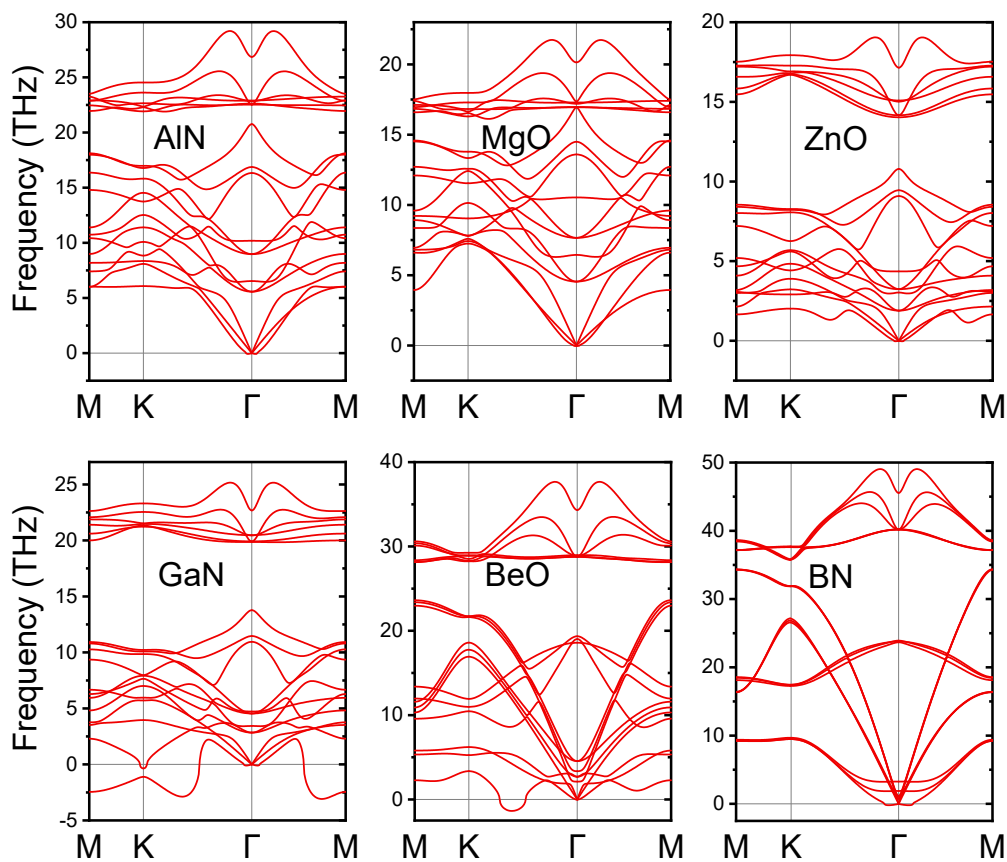
Figures

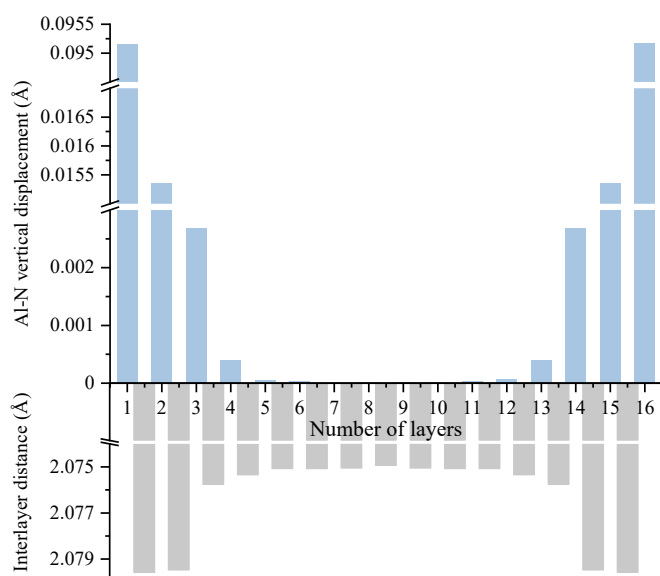Fig. S1. Phonon dispersion curves of 3-ML hexagonal rumpled films.

Fig. S2. Variation of Al-N vertical displacement (absolute values are shown) and interlayer distance with depth in a 16-ML AlN film. The interlayer distance is calculated as the distance between the in-plane bond midpoints of neighboring layers.

Structure	Rumpled hexagonal	Flat hexagonal	Wurtzite
3L AlN	$+1.35$ -1.24 / -1.38 $+1.16$ / $+1.35$ -1.24	$+1.34$ -1.25 / -1.36 $+1.17$ / $+1.34$ -1.25	-1.02 / $+1.31$ / $+1.14$ / -1.27 / $+1.09$ -1.25
4L AlN	$+1.34$ -1.22 / -1.32 $+1.20$ / $+1.20$ -1.32 / -1.22 $+1.34$	$+1.33$ -1.24 / -1.31 $+1.22$ / $+1.22$ -1.31 / -1.24 $+1.33$	-1.02 / $+1.32$ / $+1.21$ / -1.28 / $+1.17$ -1.24 / -1.27 / $+1.10$
3L ZnO	$+1.40$ -1.37 / -1.40 $+1.36$ / $+1.40$ -1.37	$+1.39$ -1.38 / -1.41 $+1.38$ / $+1.39$ -1.38	-1.19 / $+1.46$ / $+1.36$ / -1.37 / $+1.09$ -1.34
4L ZnO	$+1.39$ -1.36 / -1.38 $+1.35$ / $+1.35$ -1.38 / -1.36 $+1.39$	$+1.38$ -1.36 / -1.38 $+1.36$ / $+1.36$ -1.38 / -1.36 $+1.38$	-1.17 / $+1.46$ / $+1.36$ / -1.37 / $+1.35$ -1.37 / -1.33 / $+1.07$

Fig. S3. Mulliken charges (in units of $|e|$) of 3- and 4-ML AlN and ZnO slabs with rumpled and perfectly flat configurations. Those of the wurtzite slabs with 3- and 4-bilayer thicknesses are also shown for comparison. The pink (blue) spheres represent Al (N) atoms, and the grey (red) spheres represent Zn (O) atoms.
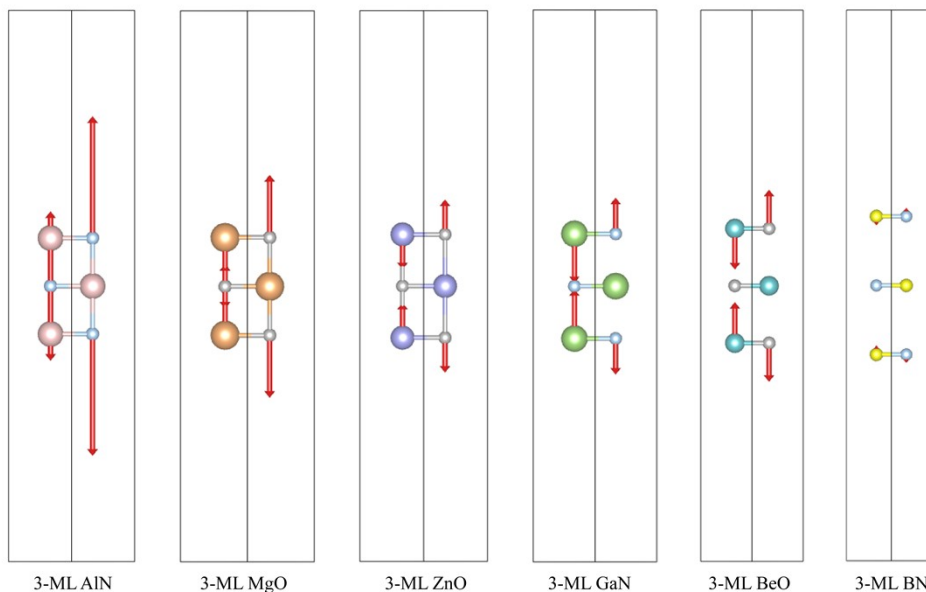
Fig. S4. Calculated Hellmann-Feynman forces for perfectly flat 3-ML hexagonal films. The arrows show the direction and amplitudes of the calculated forces on each atom.
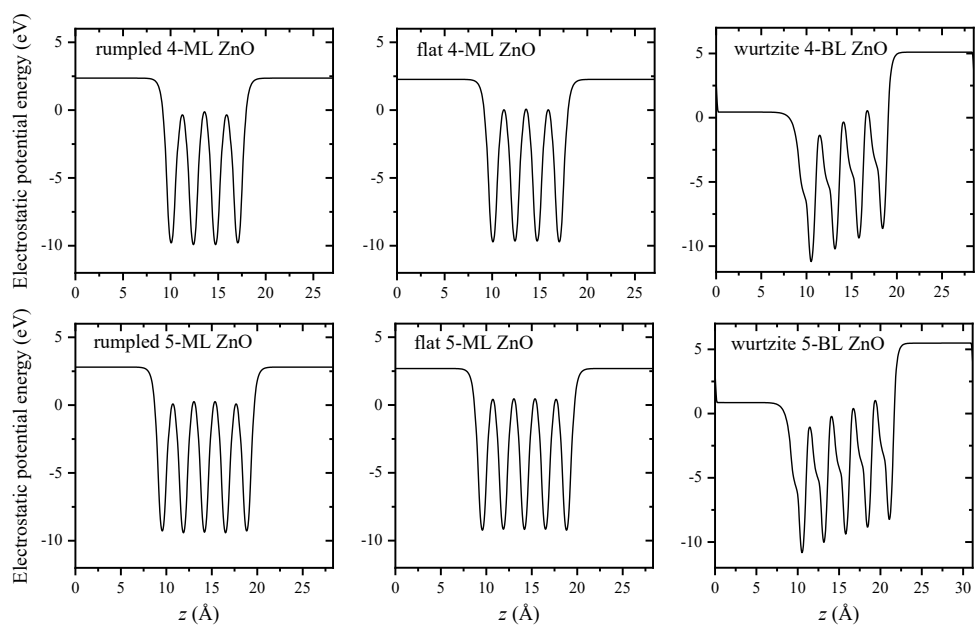

Fig. S5 Electrostatic potential curves for 4- and 5-ML ZnO slabs with rumpled and perfectly flat hexagonal structures. Those of the wurtzite slabs with 4- and 5-bilayer (BL) thicknesses are also shown for comparison.
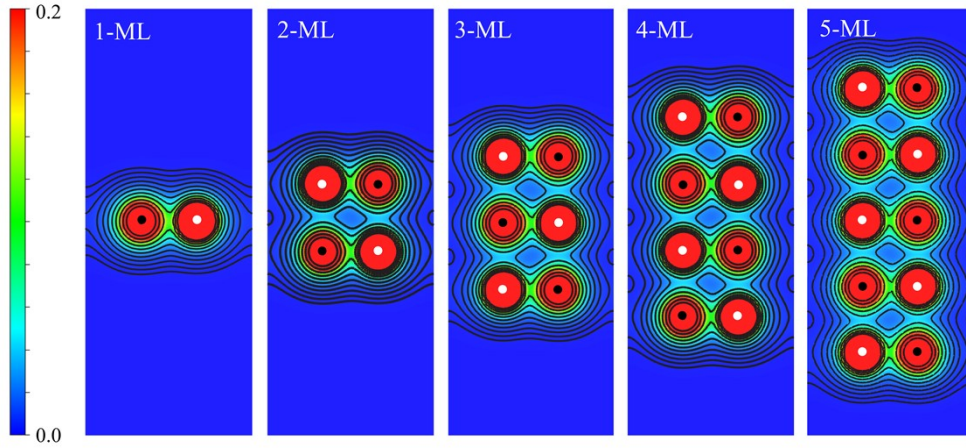
Fig. S6 Contour plots of calculated charge densities (in e/Bohr^3) in the (110) plane for perfectly flat 1–5-ML ZnO slabs. Color scale is shown on the left. Adjacent contour lines differ in charge density by a factor of $\sqrt{3}$. Nuclear positions of anions and cations are marked by black and white circles, respectively.
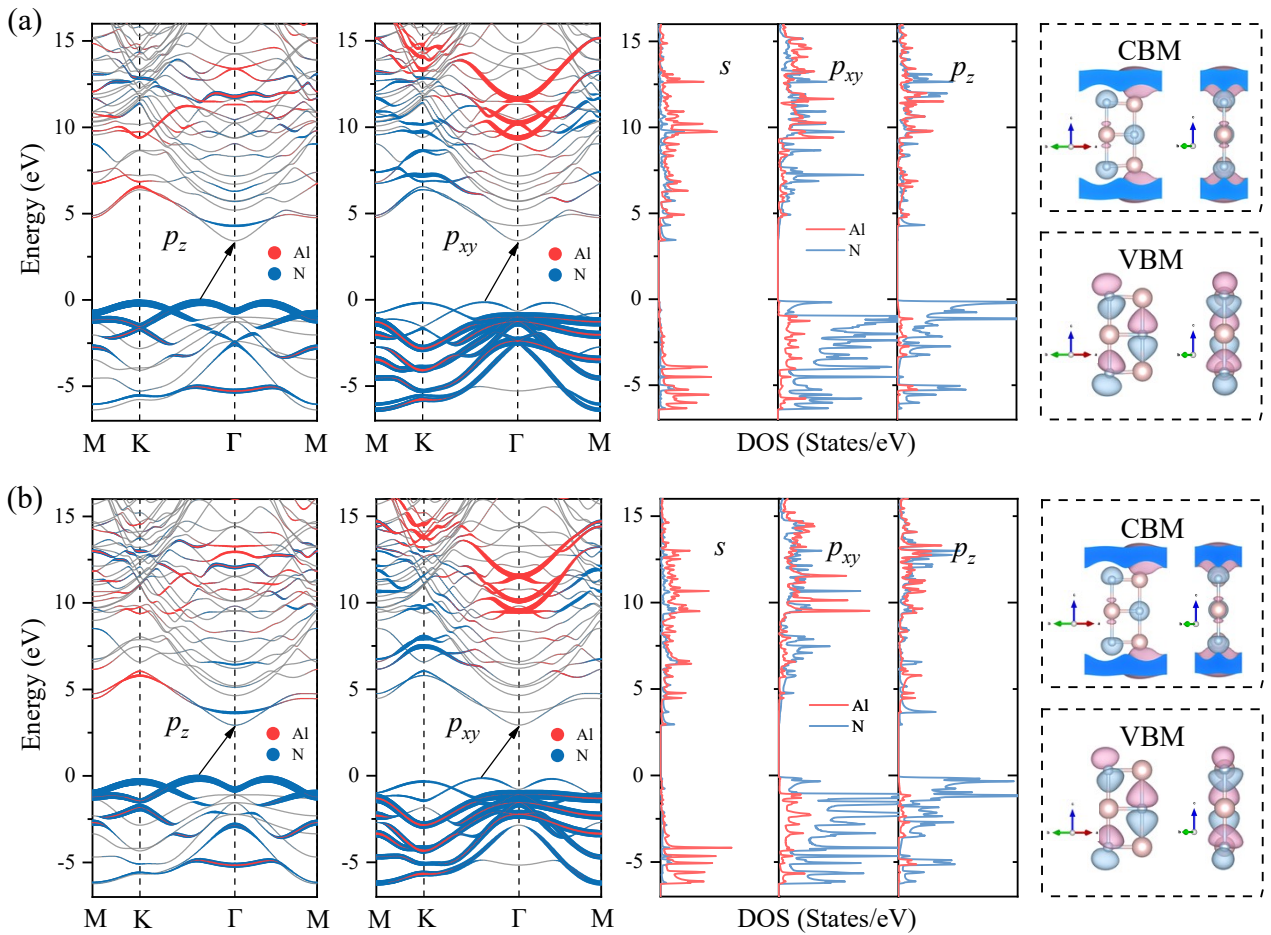

Fig. S7. Projected band structures, partial density of states, and CBM and VBM wavefunctions for (a) rumpled and (b) perfectly flat 3-ML AlN films. For the projected band structures, the radii of the red and blue circles are proportional to the Al-p_z (or p_{xy}) and N-p_z (or p_{xy}) character, respectively.

Tables

Table S1. Bond lengths and –ICOHP (up to the Fermi energy) of orbital-pair interactions in rumpled and perfectly flat 3-ML AlN films. The associated atom pairs are labeled with A–G [see Figure 7(d)].

Orbital-pair interactions	Bond length (Å)	–ICOHP (eV)
In rumpled film		
Intralayer Al(sp^2)-N(sp^2) (A)	1.861	4.602
Intralayer Al(p_z)-N(p_z) (A)	1.861	0.406
Intralayer Al(sp^2)-N(sp^2) (B)	1.859	4.298
Intralayer Al(p_z)-N(p_z) (B)	1.859	0.220
Interlayer Al(p_z)-N(p_z) (C)	2.068	0.648
Interlayer Al(p_z)-N(p_z) (D)	2.163	1.174
In perfectly flat film		
Intralayer Al(sp^2)-N(sp^2) (E)	1.859	4.526
Intralayer Al(p_z)-N(p_z) (E)	1.859	0.404
Intralayer Al(sp^2)-N(sp^2) (F)	1.859	4.272
Intralayer Al(p_z)-N(p_z) (F)	1.859	0.223
Interlayer Al(p_z)-N(p_z) (G)	2.120	0.613

Rumpled structures of thicker hexagonal films

As pointed out by Ref. [1], the critical number of layers up to which the hexagonal film is more stable than the wurtzite film is 24 for AlN. We carry out structural relaxation for a 16-ML hexagonal film of AlN. Compared with the few-layer films discussed above, the interior of this thicker film tends to be more bulklike, but the presence of surfaces can still induce structural distortions, including rumpling and changes in interlayer distance, etc. For the relaxed 16-ML slab, the variation of the Al-N vertical displacement (a measure of rumpling degree) and the interlayer distance with depth is shown in Figure S2. On the two outermost layers of the slab, the outward (inward) displacement of N (Al) atoms is

observed, leading to a rumpling of 0.095 Å, close to that of the few-layer films. The rumpling of interior layers occurs with reduced degrees and alternating signs. The rumpling degrees decrease away from the surface, and the rumpling dies out (< 10^{-4} Å) in about the fifth layer. It is clear that the rumpling of the upper four layers is repeated in the lower four layers (with opposite signs), with eight flat layers sandwiched in between (note that the atomic layers in bulk h-AlN are perfectly flat, see Ref. [2]), suggesting a symmetric configuration. Also noteworthy is that the interlayer distance decreases with depth, and its variation not only occurs on the outer layers but persists into the slab interior, with the distance between the innermost layers 8 and 9 being the shortest (2.075 Å), close to the bulk value of 2.065 Å [2]. The distribution of the interlayer distance is also symmetric around the slab center. Thus, at a larger thickness (below the critical number of layers), the hexagonal slab still adopts a symmetric configuration which gives rise to a zero total dipole moment, as is the case of the few-layer films.

Bonding characters of rumpled and perfectly flat films

Due to their structural dissimilarity, the rumpled and perfectly flat films are expected to exhibit different bonding characters. It is well known that the COHP analysis is an effective technique to investigate bonding information in the framework of DFT [3-5]. Based on auxiliary local basis sets, COHP offers a straightforward insight into orbital-pair interactions by partitioning the band-structure energy into bonding, antibonding, and nonbonding contributions. Energy-resolved –COHP curves can be derived from weighting density of states (DOS) with the associated Hamiltonian matrix element and adopt positive (negative) values for bonding (antibonding) contributions. In analogy to DOS, of which the integration up to the Fermi energy gives the number of electrons, the integrated COHP (ICOHP) can serve as a measure of bonding strength [4]. The results of the COHP analyses for the rumpled and perfectly flat 3-ML AlN films are presented in Figure 7 and Table S1. As expected, the lower valence states are dominated by the characteristic Al(sp^2)-N(sp^2) interactions (σ bonds). For higher valence states (near the Fermi energy), we observe the contribution from the intralayer Al(p_z)-N(p_z) interactions (π bonds). Above the conduction band minimum (CBM), the π* antibonding states are lower in energy than the σ* antibonding states. Interestingly, the interlayer Al(p_z)-N(p_z) interactions

also have substantial contributions to the higher valence states, with even larger –COHP and –ICOHP values than those of the intralayer π bonds. This demonstrates that in the AlN films, the interlayer overlap between the p_z orbitals along the vertical direction is more favorable than the intralayer overlap, leading to strong interlayer bonds with considerably higher bonding strength than intralayer π bonds (see the bonding schemes in Figure 7d). Such bonding character of the AlN films is intermediate between those of monolayer (with π bonds) and bulk (in which strong interlayer p_z bonds exist and π bonds are absent) h-AlN reported in our earlier work [2]. For the films of other materials, intralayer sp^2-σ bonds also exist. Going from AlN to BN (see Figure 5), as interlayer distances increase and interlayer interactions diminish from interlayer bonds to vdW forces, the predominant p_z-orbital interactions evolve from interlayer bonds (interlayer overlap) to π bonds (intralayer overlap).

In comparison with the perfectly flat film of AlN, all the orbital-pair interactions in the rumpled film exhibit higher –COHP (in particular near the Fermi energy) and –ICOHP values and thus have higher bonding strength. This holds whether the corresponding bond length in the rumpled film is larger or smaller than (or equal to) its counterpart in the perfectly flat film (see Table S1). The only exception is the subsurface intralayer π bond in the rumpled film which has merely slightly lower –ICOHP than that in the perfectly flat film, but this should not distort our conclusion. It appears that the increases in –COHP and –ICOHP of intralayer σ and π bonds from the perfectly flat to the rumpled film are relatively modest, whereas those of interlayer p_z bonds increase significantly. This suggests that the orbital interactions along the vertical direction are far more sensitive to the relative vertical displacement of cations and anions than those along the in-plane direction. The –COHP curves of the interlayer bond in the perfectly flat film (associated with the atom pair G) exhibit considerable destabilizing antibonding contributions just below the Fermi level, indicating the bonding instability. For the rumpled film, however, the overall magnitudes of the –COHP curves of the interlayer bonds, whether with a shorter (associated with the atom pair C) or a longer bond length (associated with the atom pair D), are significantly larger, and in particular, the destabilizing antibonding contribution for the longer bond appears negligible. This implies considerably higher –ICOHP values and bonding

strength for both the longer and shorter interlayer bonds in the rumpled film which are 0.561 and 0.035 eV higher than that in the perfectly flat film, respectively. This also accounts for the significant band-gap difference between the rumpled and perfectly flat films, as will be discussed below. The analyses of bonding characters again demonstrate the greater stability of the rumpled configuration relative to the perfectly flat one.

Electronic structures of rumpled and perfectly flat films

Figure S7 displays projected band structures, partial DOS (PDOS), as well as the CBM and valence band minimum (VBM) states of rumpled and flat 3-ML AlN films. A variety of rumpling-induced changes can be observed. Most striking is that the band gap of the rumpled film (3.56 eV) is 0.49 eV larger than that of the perfectly flat film (3.07 eV). This significant band-gap difference can be accounted for by the considerably lower band-structure energy of the interlayer bonds in the rumpled film than those in the perfectly flat one, as suggested by the above COHP analyses. Both the rumpled and perfectly flat films have indirect band gaps with the CBM at Γ, and the VBM appears at 0.35 (0.38) $|\Gamma K|$ away from Γ along the Γ-K direction for the former (latter). As a reflection of their intermediate bonding character, the VBM locations for the few-layer AlN films are in between the two extreme cases: bulk (with CBM and VBM at Γ and resulting direct band gap) and monolayer h-AlN (with VBM at K) [2]. Below the VBM for both films, as shown by the projected band structures, while the highest p_z band lies above the p_{xy} bands, it exhibits the same sign of curvature as the lower p_z bands (with minima at Γ), again manifesting their intermediate bonding character between bulk (whose higher p_z band has a maximum at Γ, as opposed to the lower p_z band, indicating strong p_z-orbital interactions along the vertical direction) and monolayer h-AlN (whose p_z band is lower than the p_{xy} bands and has a minimum at Γ, typical of π bonding) reported in our earlier work [2].

Compared with the perfectly flat film, the highest p_z band of the rumpled film exhibits a slightly smaller curvature, which is indicative of the increased strength of interlayer p_z bonds. This is consistent with the above COHP analyses and is the reason why the VBM of the rumpled film is slightly nearer to Γ. Moreover, the valence bands of the rumpled film exhibit narrower splittings at Γ. For example, a p_z

band (with minima at Γ) and two p_{xy} bands (with maxima at Γ) of the rumpled film are nearly degenerate around -2.5 eV at Γ, leading to a branched shape, while for the perfectly flat film, a gap of ~0.6 eV appears between two p_{xy} bands.

The VBM of the rumpled film shows predominantly p_z character with a small p_{xy} component. Similar contributions can be observed for the VBM of the perfectly flat film but with slightly reduced magnitude. Their CBMs all exhibit parabolic dispersion, very low DOS (with small Al- and N-s components), and thus the free-electron-like surface character. This is a common feature of layered materials such as graphene, graphite, h-BN as well as monolayer h-AlN [2,6-9]. As shown by the PDOS and the isosurface plots of 3-ML AlN in Figure S7, the CBM electrons are mainly concentrated outside both surfaces of and nearly parallel to the films, similar to the case of monolayer h-AlN but distinct from the bulk where the CBM electrons are confined in the channels perpendicular to the atomic planes (termed channel states, see Ref. [2]). Compared with the perfectly flat film, the surface N atoms of the rumpled film are displaced slightly outwards relative to the surrounding CBM electrons (with N-s character), while the surface Al atoms inwards relative to the outer CBM electrons (with free-electron-like character). For the VBM of the rumpled film, the p_z-like orbitals of the surface N atoms are symmetric about the (110) plane, whereas asymmetry is observed for those in the perfectly flat film. This may account for the higher bonding strength and stability of the rumpled configuration.

References

[1] C. L. Freeman, F. Claeyssens, N. L. Allan, and J. H. Harding, Phys. Rev. Lett. **96**, 066102 (2006).

[2] A.-A. Sun, S.-P. Gao, and G. Gu, Chem. Sci. **11**, 4340 (2020).

[3] S. Maintz, V. L. Deringer, A. L. Tchougréeff, and R. Dronskowski, J. Comput. Chem. **37**, 1030 (2016).

[4] V. L. Deringer, A. L. Tchougréeff, and R. Dronskowski, J. Phys. Chem. A **115**, 5461 (2011).

[5] S. Maintz, V. L. Deringer, A. L. Tchougréeff, and R. Dronskowski, J. Comput. Chem. **34**, 2557 (2013).

[6] N. A. W. Holzwarth, S. G. Louie, and S. Rabii, Phys. Rev. B **26**, 5382 (1982).

[7] M. Posternak, A. Baldereschi, A. J. Freeman, and E. Wimmer, Phys. Rev. Lett. **52**, 863 (1984).

[8] X. Blase, A. Rubio, S. G. Louie, and M. L. Cohen, Phys. Rev. B **51**, 6868 (1995).

[9] A. Catellani, M. Posternak, A. Baldereschi, and A. J. Freeman, Phys. Rev. B **36**, 6105 (1987).